Receptors and Enzymes for Medical Sensing of L-Glutamate

Ayumi Hirano[1] and Masao Sugawara[2,*]

[1]*Division of Neurophysiology, National Institute for Medical Research, London, NW7 1AA, UK;* [2]*Department of Chemistry, College of Humanities and Sciences, Nihon University, Tokyo 156-8550, Japan*

Abstract: Medical sensing systems using isolated or intact glutamate receptor (GluR) ion channels and glutamate oxidase (GluOx) are discussed for L-glutamate, one of the principal neurotransmitter in the central nervous systems of mammalian brain, and related agonists. The GluR-based sensing system used for the evaluation of signal transduction ability of GluR channels demonstrate that the agonist selectivity based on the signal transduction ability is not parallel to that of the binding assay. On the other hand, the appropriate design of the enzyme system, namely glutamate oxidase (GluOx), in combination with horseradish peroxidase (HRP), enables to real-time monitoring of L-glutamate *in vivo* and *in vitro* and also to visualize its release in submerged, acute mouse hippocampal slices.

Key Words: Glutamate receptor ion channels, Glutamate oxidase, acute brain slice, agonist selectivity, patch sensor, visualization of glutamate release, micro sensor.

INTRODUCTION

L-Glutamate is a major excitatory amino acid neurotransmitter in the central nervous systems of mammalian brain and thought to play a crucial role in brain development, synaptic plasticity and neurotoxicity [1,2]. The development of highly sensitive and selective sensing methods for L-glutamate is therefore important for understanding the role of L-glutamate both in physiological and pathological processes in brain on the basis of its spatial and temporal distribution. For designing L-glutamate sensors, glutamate receptor (GluR) ion channels and glutamate oxidase (GluOx) are attractive compounds as biological sensing elements for L-glutamate (Tables **1** and **2**). The high affinity (~nM) [3] and fast response (~ms) [4] of GluRs to L-glutamate enables to design a highly sensitive L-Glutamate sensor with fast response time, although the activity of GluRs is available only if GluRs are incorporated in lipid bilayer matrices, such as planar bilayer lipid membranes (BLMs), liposomes and cell membranes [5]. On the other hand, the enzyme activity of GluOx is more robust, which enables us the designs of versatile sensors using GluOx dissolved in an aqueous solution [6,7] or immobilized on a solid support, including an electrode [8,9]. The uses of the biological sensing elements for the design of L-glutamate sensing systems provide novel approaches for medical sensing of L-glutamate in brain and brain slices. In this review, we focus on new approaches for L-glutamate sensing in brain slices based on GluRs and GluOx.

GLUR CHANNELS IN PLANAR BLMS FOR SENSING OF L-GLUTAMATE

In the early 1990's, a reliable procedure was developed for an active preparation of a glutamate receptor (GluR) ion channel containing several essential components including the 71-kDa glutamate binding glycoprotein [10]. By using the procedure with a slight modification, we got a GluR protein suspension containing 71-, 42-, and 36-kDa protein and 58-kDa protein from rat whole brain [11]. The GluR protein as a sensing element for L-glutamate was incorporated with an artificial bilayer lipid membrane (BLM) and the reconstituted system was used as a sensor for detecting agonists [11-13]. The purified GluRs were necessary to be fused with planar BLMs formed by the so-called folding and tip-dip methods. Consequently, depending on the number of receptors that are spontaneously fused in BLMs, the sensors were classified into two groups, i.e., single- and multi-channel sensors.

In the single-channel sensor where a BLM contains an active single GluR channel, the sensor exhibits its response as repetition of a rectangle-shaped current pulse, each one corresponding to transition between the open and closed states of the single-channel in the BLM. Both the frequency of channel openings [12] and the integral of the single-channel current [11] are relevant signals for measuring the concentration of L-glutamate in solutions. The integrated current-based sensor is more sensitive to L-glutamate than the frequency-based one, the dynamic range covering 1-3 μM for the integrated current-based sensor and 50−500 μM for the frequency-based one. Since the BLM contains an active single-channel, the very magnitude of the integrated single-channel current can be compared among different BLMs, and therefore the ability of each GluR channel to transport ions is obtained directly from the integrated current [14].

In the multi-channel sensor, the channel current is the sum of all single-channel currents generated by GluRs in the BLMs. The observed currents are much larger than those with the single-channel sensor, leading to higher sensitivity to L-Glutamate. By using an integrated multi-channel current as an output signal, the sensor could detect L-glutamate at the concentration of as low as 0.10 nM [13]. However, in this approach, the numbers of receptors in BLMs vary from one membrane to another. Consequently, a relative magnitude of

*Address correspondence to this author at the Department of Chemistry, College of Humanities and Sciences, Nihon University, Tokyo 156-8550, Japan; E-mail: sugawara@chs.nihon-u.ac.jp

1389-5575/06 $50.00+.00

Table 1. L-Glutamate Sensors Based on GluOx, GluRs and Glutamate Transporter Applied to Neuronal Samples

Sensor structure	Sensory element for L-Glu	Detection	Sample	Stimulation	Ref.
(a) glutamate oxidase (GluOx)					
Dialysis electrode	GluOx, in solution	oxidation at Pt	*in vivo*, rat striatum	tail pinch	[6]
Dialysis electrode	GluOx, in solution	oxidation at Pt	*in vivo*, rat hippo-campus	electrical	[7,63]
Dialysis electrode	GluOx, in solution	oxidation at Pt	*in vivo*, rat striatum	ischemia	[67]
Dialysis electrode	GluOx, in solution	oxidation at Pt with mediator ferrocene	*in vivo*, rat striatum	anoxia	[68]
Capillary electrode	GluOx in solution	reduction at Os-gel-HRP-modified Pt	acute hippocampal slices	K^+ (200 mM) ischemia	[65,66]
Microdialysis	GluOx, immobilized (Gelatin, BSA/glutaraldehyde)	oxidation at Pt	*in vivo*, rat striatum and cortex	cardiac arrest, K^+ (100-160 mM) electrical	[61,62]
Microdialysis	GluOx, immobilized (BSA/glutaraldehyde)	reduction at Os-gel-HRP-modified GC	cultured nerve cells	K^+ (100 mM)	[64]
Electrode array	GluOx, immobilized (HRP, Os hydrogel, PEGDGE on Au)	reduction	cultured nerve cells	K^+ (100 mM)	[9]
Electrode array	GluOx, immobilized (BSA/glutaraldehyde on Os-gel-HRP-modified ITO)	reduction	hippocampal slice cultures	muscimol (1 mM) electrical	[38,54]
Micro-capillary sam-pling	GluOx, immobilized (BSA/glutaraldehyde on Os-gel-HRP modified GC)	reduction	cultured nerve cells	K^+ (100 mM)	[8]
Microsensor	GluOx, immobilized (BSA/glutaraldehyde on Pt-Ir)	oxidation	*in vivo*, rat hippo-campus	K^+ (100 mM) electrical	[71]
Microsensor	GluOx, immobilized (HRP, Os hydrogel, PEGDGE on CF)	reduction	*in vivo*, rat striatum	TTX (100 μM)	[72]
(b) glutamate receptor ion channel (GluR)					
Patch sensor	GluRs in cell membranes	ion channel current	acute hippocampal slices	electrical	[32-34]
Patch sensor	GluRs in cell membranes	ion channel current	acute hippocampal slices	ischemia	[35]
Patch sensor	GluRs in cell membranes	integrated channel current	acute hippocampal slices	GABA(20 μM)	[36]
(c) glutamate transporter (GT)					
Patch sensor	glial GT in cell membranes	transporter current	acute hippocampal slices	electrical	[73-75]

BSA: bovine serum albumin, GC: glassy carbon, CF: carbon fiber, HRP: horseradish peroxidase.

the integrated current induced by an agonist to that by a reference agonist is relevant as a sensor signal.

AGONIST SELECTIVITY OF GLURS BASED ON ION-PERMEATION ABILITY

The agonist selectivity (potency) of receptor ion channels has been described in terms of binding affinity of agonists for the receptor [15,16]. The method for obtaining binding affinity is, in principle, based on quantification of the amount of agonists bound to the receptor channel. The potency of agonists to induce the channel activity of receptor channels is also described on the basis of agonist concentration known as half-maximum response (EC_{50}) [4,17,18]. On the other hand, the essential role of receptor ion channels in neuronal signal transmission is to allow the entry of ions such as Ca^{2+},

Table 2. Imaging of L-Glu Based on GluOx, Glutamate Dehydrogenase, GluR, Glutamate Transporter and Fluorescent Indicator Protein

Imaging reagents for L-Glu	Detection	Sample	Stimulation	Ref
(a) glutamate oxidase (GluOx)				
GluOx+HRP+DA64 (redox dye)	colorimetry	acute brain slices	K^+ (1 M) ischemia	[55,56]
GluOx+POx+Amplex™ Red (redox dye)	fluorometry	cultured nerve cells	K^+ (53.5 mM)	[76]
(b) glutamate dehydrogenase (GDH)				
GDH	fluorometry (NADH)	acute hippocampal slices	ischemia	[52]
GDH	fluorometry (NADH)	acute retinal slices	K^+ (30 mM) Basal release	[77] [78]
GDH	fluorometry (NADH)	acute spinal cord slices	K^+ (80 mM)	[79]
GDH	fluorometry (NADH)	cultured astrocytes	mechanical	[80]
(c) glutamate receptor ion channel (GluR)				
GluR-expressing cells+fura2/AM	fluorometry (Glu-induced Ca^{2+} influx)	acute hippocampal slices	ischemia	[53]
(d) glutamate transporter (GT)				
GT+RH 155 (voltage-sensitive dye)	absorptiometry (glial depolarization)	acute hippocampal slices	electrical	[81]
(e) fluorescent indicator protein for Glu (FLIPE, glutamate/aspartate binding protein ybej fused to two variants of the green fluorescent protein)				
FLIPE-expressing cells	fluorometry (FRET) POx: peroxidase	transfected cell cultures	K^+ (90 mM)	[82]

Na^+, and K^+ from the extracellular space into the cell interior, which triggers the activation of successive signaling processes. The evaluation of signal transduction ability of GluR channels in terms of the number of ions passed through the channels is, therefore, important for understanding the inherent properties of GluR channels in neuronal transmission, the development of pharmaceutical chemicals and so on.

The evaluation of agonist selectivity of N-methyl-D-aspartate (NMDA) receptor [13] and its subtypes (ε1–4/ζ1 channels) [14,19,20] based on the number of ions (coulomb) permeated through the channel has been addressed in recent reports (Fig. **1a**). Partially purified GluRs from rat whole brain were incorporated into planar BLMs and the number of ions passed through the GluR channels activated by each agonist was quantified in term of integrated channel currents (coulomb). Among typical agonists NMDA, L-glutamate and L-CCG-IV, the agonist selectivity obtained as a ratio of the integrated current induced by an agonist to that induced by a reference agonist L-glutamate (Fig. **1b**) was NMDA:L-glutamate:L-CCG-IV= 0.47:1.0:2.9 [13]. The range of the selectivity is much narrower than that determined from binding affinities (NMDA:L-Glutamate:L-CCG-IV= 0.022:1.0:17) [21]. The narrower selectivity suggests that the ability of the receptor ion channel to pass ions is not parallel to the binding affinity of the agonists.

NMDA receptors comprise both ζ1 and ε receptor subunits [4,22]. Since each channel type (ε1/ζ1, ε2/ζ1, ε3/ζ1, and ε4/ζ1, mouse forms of NR1/NR2A, NR1/NR2B, NR1/NR2C and NR1/NR2D [22]) has its own regional distribution in the brain [22,23] and exhibits its specific function [24-26], it is becoming important to evaluate agonist selectivity for each channel type. Extending the above approach to the recombinant ε1–4/ζ1 channels embedded in BLMs, the ion-permeation ability of each channel type, i.e., ε1/ζ1, ε2/ζ1, ε3/ζ1 and ε4/ζ1 channels, has been quantified with single-channel sensors for L-Glutamate, NMDA and L-CCG-IV (Fig. **1c**) [14,19]. At 50 μM agonist concentration, where the binding sites of the ε1–4/ζ1 receptor channels are expected to be fully occupied by L-glutamate on the basis of the reported EC_{50} values [23,27], the magnitudes of the integrated single-channel currents induced by L-glutamate exhibited dependence on the ε-subunit composition in the order of ε2/ζ1 > ε1/ζ1 ≈ ε4/ζ1 > ε3/ζ1 (Table **3**). The selectivity order among the four channel types is clearly different from that (ε4/ζ1 > ε3/ζ1 ≈ ε2/ζ1 > ε1/ζ1) of the ligand affinities estimated from the reported EC_{50} values of L-glutamate [23,27]. Considering the occupation of binding sites of the ε1/ζ1 and ε2/ζ1 receptors by L-Glutamate, the observed order may reflect the slower desensitization of ε2/ζ1 than ε1/ζ1 [28]. The dependence of ion permeation on ε-subunits suggests that each channel type activated by L-glutamate has its own ability of ion permeation.

The individual roles of the ε2/ζ1 and ε1/ζ1 channels in neuronal signal transmission have attracted attention in recent works, because some forms of synaptic plasticity may be regulated by ε2 and ε1 subunits [29-31]. For example,

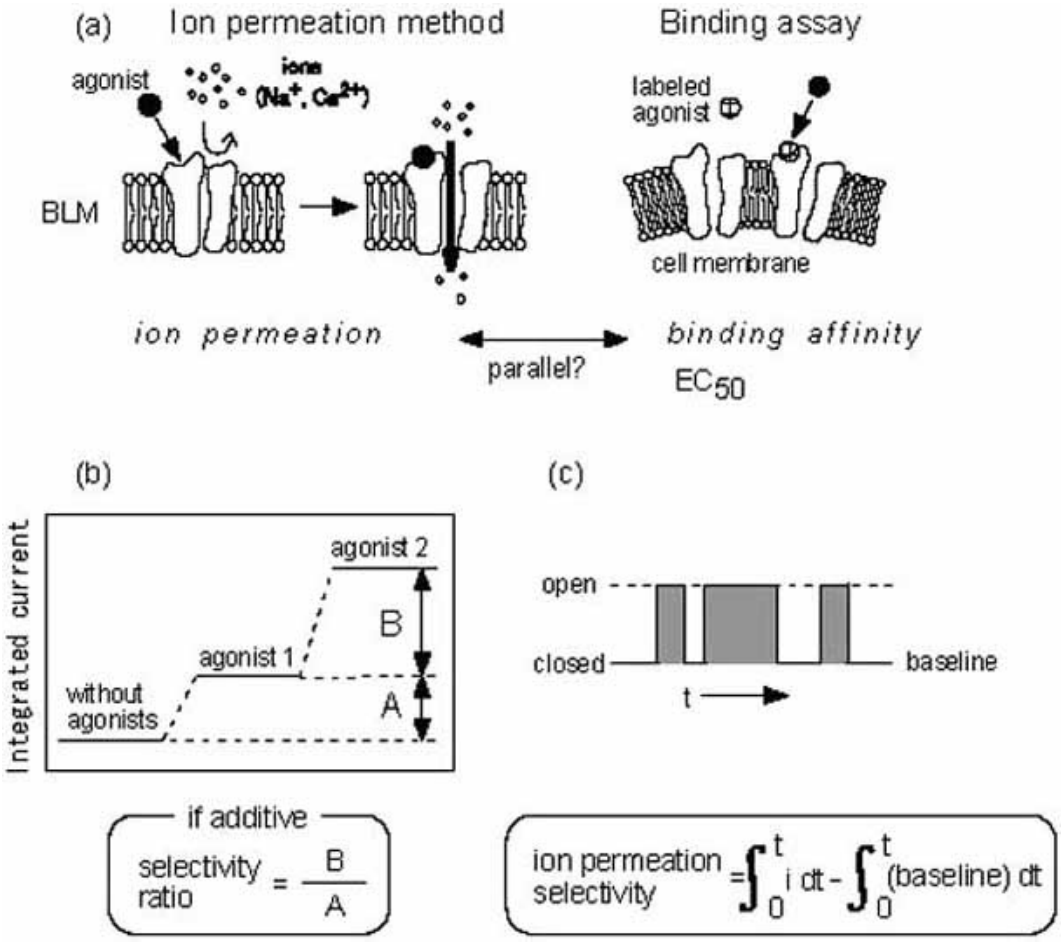

Fig. (1). Evaluation of agonist selectivity based on ion permeation ability of GluRs. (a) Comparison with binding assay. (b) Multi-channel sensor. (c) Single-channel sensor.

long-term potentiation (LTP) is mediated by NMDA receptors containing ε1 subunits, whereas long-term depression (LTD) requires activation of receptors containing ε2 subunits [29,30]. Our data show that the number of ions permeated through the ε2/ζ1 channel is greater than that through ε1/ζ1 channel at saturating concentration of L-Glutamate. The order of ε2/ζ1 > ε1/ζ1 is in agreement with that for the simulated charge transfer (ion permeation) by a single synaptic activation and repeated activation at low frequency typically used to induce LTD, but is the reverse of the order (ε1/ζ1 > ε2/ζ1) for the simulated charge transfer under high-frequency stimulation typically used to induce LTP [28].

GLURS IN BIOLOGICAL MEMBRANES FOR DETECTION OF L-GLUTAMATE

The intact GluR ion channels in cell membranes are promising bioelements for sensing L-Glutamate. By using GluRs in an excised membrane, a microsensor of 1-2 μm for L-glutamate can be constructed, by which the spatial and time resolution of L-glutamate sensing is improved. In addition, the patch sensor is expected to be highly sensitive to L-glutamate and have response time of ~ms. Such features of patch sensors are important for detection of chemical stimulant-induced glutamate release, because stimulation is usually achieved by injection or perfusion of a stimulant solu-

Table 3. Comparison of Ion Permeation Selectivity Obtained from the Single-Channel Sensor and Ligand Affinity. Data were Taken from Refs. [14 and 19]

		ε1/ζ1	ε2/ζ1	ε3/ζ1	ε4/ζ1
Ion permeation ($X 10^{-13}$ C/s)	L-Glu NMDA L-CCG-IV	5.8±0.7 4.5±0.6 6.6±0.6	7.1±0.4 4.0±1.2 4.8±1.1	3.3±0.2 4.1±0.4 5.7±0.5	6.0±0.4 3.8 6.7±0.9
Ligand affinity ($1/EC_{50}$, 10^6 M^{-1})	L-Glu	0.59	1	1	3

tion to a brain slice submerged in a bath solution and hence the sensor needs to be highly sensitive to L-glutamate locally spilled and diffused from the slice. The patch sensors for L-Glutamate, introduced by several authors [32-35], could detect micromolar concentration of L-glutamate released in hippocampal slices by electric stimulation.

By using a patch sensor with improved sensitivity, detection of GABA-stimulated release of L-glutamate at sub-μM level from various neuronal regions of acute mouse hippocampal slices has been exploited [36]. In the patch excised from cell membranes in the cornu ammonis 3 (CA3) region of hippocampal slices, both NMDA and AMPA receptors were present. However, the contribution of NMDA receptors to the response was more significant for L-glutamate at concentration of sub-μM to several μM, because NMDA receptors have higher affinity to L-glutamate than AMPA receptors [17] and hence are activated at lower concentration. The patch sensor exhibited a detection limit of 0.50 μM, which is superior to that with the patch sensor reported by Maeda *et al*. [32,33]. The GABA (25 μM) stimulation induced release of L-glutamate from the cornu ammonis 1 (CA1) and dentate gyrus (DG) regions of the hippocampal slices, but in the CA3 region, GABA induced no noticeable release of L-Glutamate. The stimulation by GABA in the presence of a $GABA_A$ receptor antagonist, bicuculline (25 μM), showed that the most part of L-glutamate release from the CA1 region occurred *via* a $GABA_A$ receptor pathway. This mechanism is in accordance with the distribution of GABA receptors in hippocampus. The high density of $GABA_A$ binding is observed in the CA1 and DG regions of the hippocampus, whereas $GABA_B$ binding sites are distributed in the CA3 [37]. The region-specific release of L-glutamate observed with a patch sensor is in agreement with the result of Kasai *et al*. who showed by using an electrode array that GABA enhances the release of glutamate in the CA1 and DG regions of cultured hippocampal slices when $GABA_A$ receptors were activated [38].

GLUOX-BASED MEMBRANES FOR IMAGING OF L-GLUTAMATE RELEASE

Visualization of regional distribution of L-glutamate release in brain slices is important for understanding physiological and pathological actions of L-Glutamate, because neurons in different regions, for example, CA1, CA3 and DG in the hippocampus exhibit different behavior in response to the same physiological stimulation [39,40]. In contrast to intracellular messengers for which versatile imaging methods have been reported [41-47], a limited number of studies have been described on imaging the distribution of extracellular neurotransmitters [48-51]. Only several approaches have been exploited for imaging L-glutamate released in brain slices, including fluorometric methods using glutamate dehydrogenase [52] and fura 2-loaded CHO cell lines expressing NMDA receptors [53] and an electrochemical method using an electrode array modified with GluOx and horseradish peroxidase (HRP) [38,54]. However, all of them failed to visualize regional distribution of L-glutamate release in the hippocampus due to insufficient spatial resolution.

The improvement of spatial and time resolution for visualizing L-glutamate release in an acute brain slice has been achieved by using an enzyme membrane composed of GluOx and HRP immobilized in a bovine serum albumin-glutaraldehyde matrix on a poly(L-lysine)-coated cover slip [55]. When a brain slice, after loaded with a dye DA-64 (a substrate for HRP), is placed on the membrane, the enzymes diffuse spontaneously from the membrane into the extracellular fluid of the brain slice, where L-glutamate spilled from neurons triggers enzymatic conversion of DA-64 to Bindschedler's Green (BG) (Fig. **2a**). In the proof-of-concept study with an GluOx-HRP membrane, the regional distribution of depolarization (0.20 M KCl)-induced L-glutamate release in the hippocampus of a mouse brain slice was visualized (Fig. **3a**), although the visual image was a time-integrated one rather than a time-resolved image [55].

A difference-image analysis with the GluOx-HRP membrane has overcome the shortcoming of the enzyme-based approach [56]. The difference-image analysis, as shown in Fig. **2b**, gives a slope of measured color signals, which is proportionally related to a flux (mol min^{-1} cm^{-2}) of L-glutamate. Hence, not only an increase but also a decrease in the L-glutamate flux can be imaged. The spatial resolution of the enzyme membrane method is 42 μm, which is better than that (71-92 μm) of the CHO cell-based approach [53] and that (~50 μm) of the enzyme-modified electrode array [38, 54].

Time-resolved imaging of hippocampal distribution of ischemia-induced L-glutamate release in mouse brain slices has been addressed by using a difference-image analysis [56]. Brain ischemia is known to cause neuronal cell death in the hippocampus [57,58]. It is considered that ischemia-induced cell death is mediated by excessive release of L-glutamate in the extracellular space and subsequent activation of glutamate receptors in postsynaptic cells [57,58]. Upon the onset of ischemia, an intense signal that indicates release of L-Glutamate, originated in the stratum orien of the CA3 region and extended into the CA1 and DG regions (Fig. **3b**). The signals in the CA1 and DG regions then are weakened. At 7.7 min after the onset of ischemia, the flux (nmol min^{-1} cm^{-2}) of L-glutamate was in the order of CA1 ≈ CA3 > DG.

GLUOX IMMOBILIZED IN A GLASS CAPILLARY FOR DETECTING L-GLUTAMATE

Another useful approach for detecting L-glutamate release in brain slices is the use of a microsensor of ~μm size. As discussed above, the imaging methods have the advantage that L-glutamate release in brain slices can be simultaneously monitored at multiple points. However, addition of imaging reagents such as fluorescence dyes, in our case a coloration dye, and enzymes into the target systems are necessary for visualizing a colorless or non-fluorescent neurotransmitter like L-Glutamate. Consequently, chemical perturbation of the target system cannot be neglected. On the other hand, an approach using a microsensor provides less perturbed, quantitative information on L-glutamate concentration, although concentration of a target compound is usually obtained only at a local, single point close to the sensor surface. Imaging and microsensor methods, therefore, complement each other.

Many L-glutamate sensors based on large-volume sampling techniques, for example, microdialysis combined with various analytical methods have been developed and used for

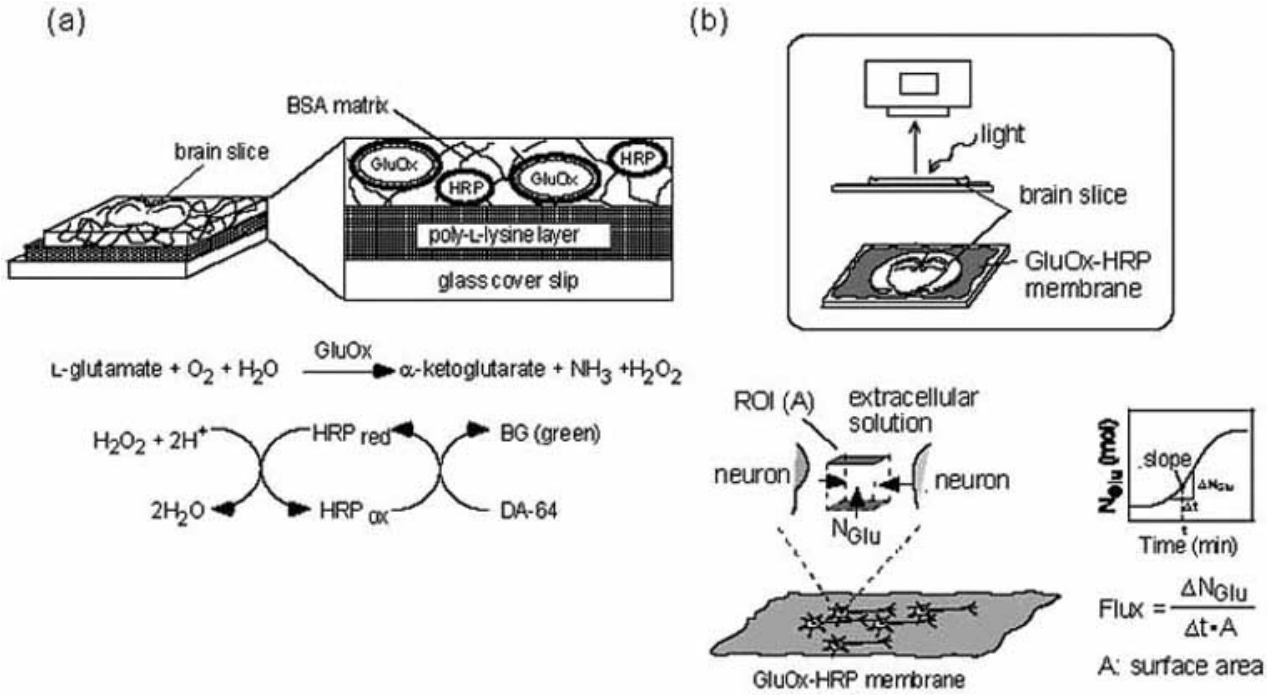

Fig. (2). Schematic illustration for the principle of (a) color imaging of L-glutamate released from mouse-brain slices and (b) difference-image analysis.

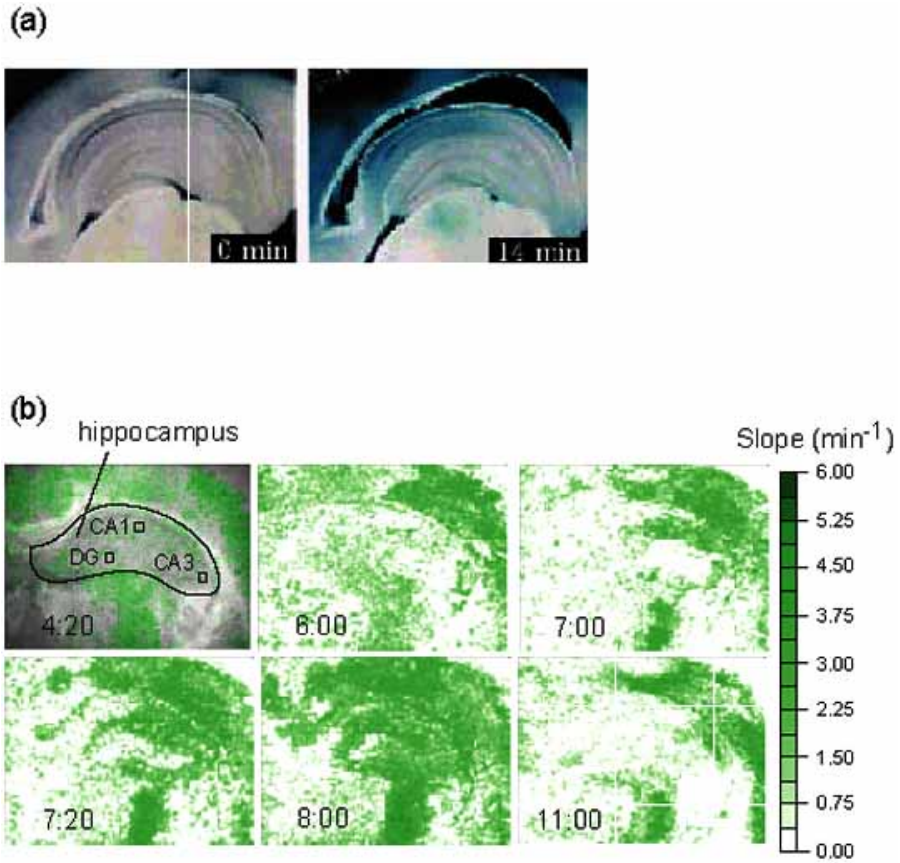

Fig. (3). (a) Color images for coronal mouse brain slices under 1 M KCl stimulation. (b) Time-resolved two-dimensional visual images of L-glutamate fluxes in a mouse coronal slice during ischemia.

in vivo [6,7,59-63], cultured neurons [8,9,64] and organotypic slice cultures [38,54]. However, real time monitoring of L-glutamate in acute brain slices, which is one of the most common samples used for brain research, have not been established yet. To develop L-glutamate sensor applicable to acute brain slices, minimizing the size of the sensing probes is essential, because the volume of acute slices is very small (~2 μl for a 300-μm thick mouse hippocampal slice). The small size of the probes is also favorable because L-glutamate release is highly localized in extracellular fluid. In addition, using a small probe can minimize physical and chemical perturbations of the target system.

For the purpose of minimizing the size of the sensing probes, pulled glass capillaries have unique features. The tip diameters range from submicro- to several μm, capillarity at the tip works as a small-volume sampling mechanism and the glass surface has biocompatibility. In addition, the inner space of a glass capillary provides a reservoir for a solution containing enzymes, in the present case GluOx and L-ascorbate oxidase (AsOx), and an electrochemical transducer [65] (Fig. **4a**). The capillary action at the open tip (10 μm) can sample a very small volume (~55 nl/min) of a buffer solution containing L-glutamate into the inner solution, but in a buffer solution 60 μm above a hippocampal slice, the sampling rate drops to ~3.5 nL/min [66], because the solution viscosity was increased by a leak of cellular components from the acute slice. The sampling rate is much slower than that (0.5 μL/min) with a dialysis electrode [67,68] and those (4 μL/min) with a microdialysis technique [64] and a glass capillary in a suction mode [8].

In the proposed L-glutamate sensor system [65,66], the enzyme reaction of GluOx within the electrode generates electroactive hydrogen peroxide, which is detected at an underlying Os-gel-HRP modified electrode [69,70].

$$\text{L-glutamate} + O_2 + H_2O \rightarrow \alpha\text{-ketoglutarate} + NH_3 + H_2O_2 \quad (1)$$

$$2Os(II) + H_2O_2 + 2H^+ = 2Os(III) + 2\,H_2O \quad (2)$$

$$Os(III) + e = Os(II) \quad (3)$$

The response profile of the capillarity-based sensor for L-Glutamate (Fig. **4b**) is similar to those of the conventional amperometric sensors, though the response mechanism was essentially different. The reason why a steady current is attained, irrespective of continuous inflow of L-Glutamate solution is that an increase in the concentration of hydrogen

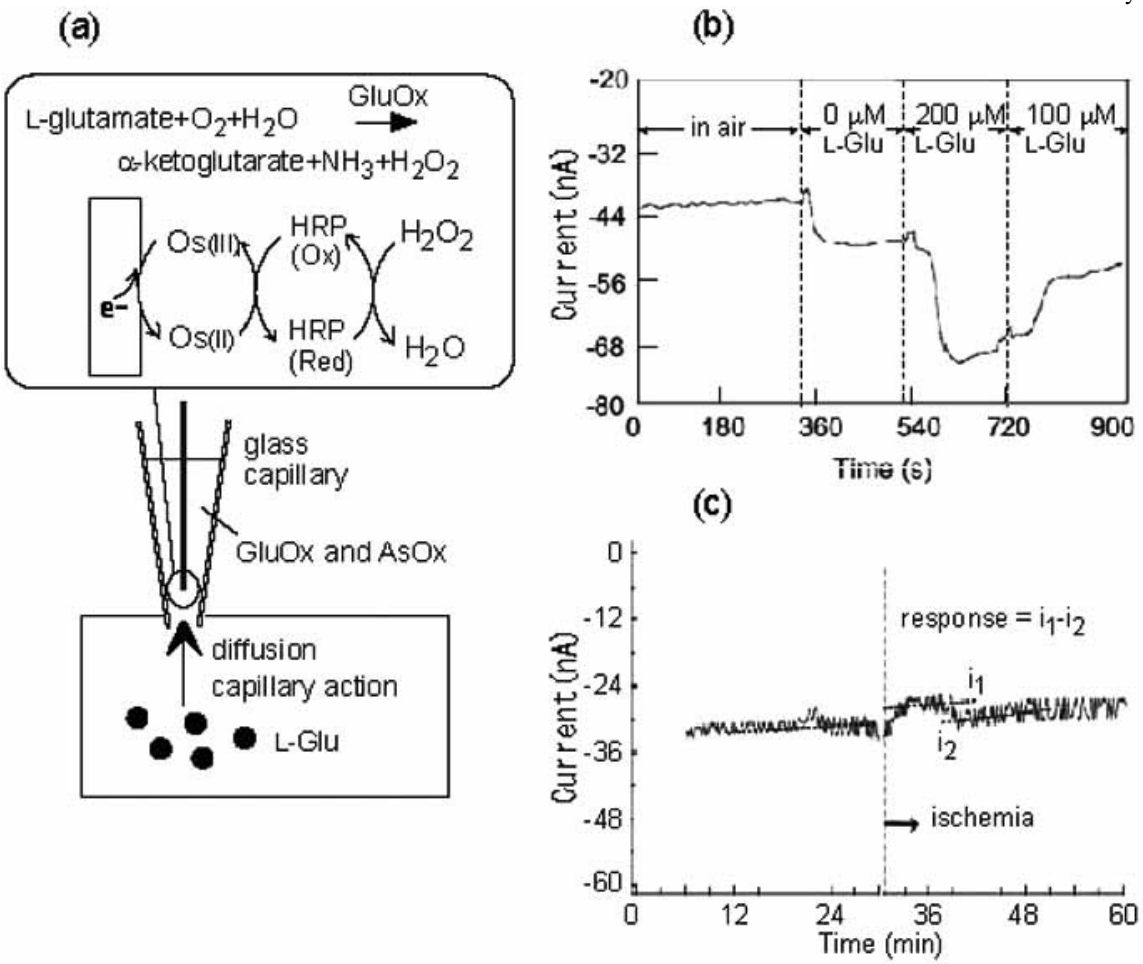

Fig. (4). (a) Schematic illustration for the principle of the capillary-based sensor for L-glutamate. (b) Time-course of the amperometric current at the capillary electrode. (c) An example of current traces for ischemia-induced L-glutamate release. The operational potential was 0 mV *vs*. Ag/AgCl.

peroxide produced by the enzyme reaction of L-Glutamate in a small volume of the inner solution is counterbalanced by consumption of hydrogen peroxide at the electrode, leading to a steady concentration of hydrogen peroxide. Importantly, the response to L-Glutamate is reversible and hence the sensor detects not only an increase but also a decrease in L-Glutamate concentration. The response is highly selective to L-Glutamate over ascorbate, dopamine, serotonin and other amino acids, by virtue of the specific enzyme reactions by GluOx and AsOx and a low applied potential of 0 mV *vs*. Ag-AgCl.

The capillary electrodes have been applied to detection of L-Glutamate release in mouse hippocampal slices stimulated by depolarization (0.10 M KCl) [65] and hypoxia (Fig. **4c**) [66]. The KCl-evoked L-Glutamate release increased in the order of DG ≈ CA3 > CA1 (below detection limit), in accordance with the *in vivo* results with a dialysis electrode reported by Bliss's group [63] and the results of slice experiments with a patch sensor reported by Maeda *et al*. [33]. On the other hand, the order of CA1 ≈ CA3 > DG for the L-Glutamate release during ischemia is in accordance with that of the L-Glutamate flux during ischemia obtained by the difference imaging method described above [56].

COMPARISON OF THE PROPOSED METHODS

In Table **4** the response features of the proposed sensing methods for L-glutamate are summarized. The BLM sensors based on multi GluR channels (case a) are highly sensitive to L-Glutamate, though the method is relied on the isolated GluRs and comparison of the responses has to be done within a single BLM. On the other hand, the responses of the micro BLM sensors based on a single GluR (case b) can be compared between different sets of the BLMs, but the sensitivity is lowered. While these artificial BLM-based sensors are useful for *ex situ* experiments with isolated receptors, the biomembrane sensors (case c) are adaptable to *in situ* experiments, especially targeted toward elucidating neuronal activities. The biomembrane sensors have the sensitivity that matches the concentration of L-glutamate (~sub μM) released in brain slices by chemical stimulation. The fragile nature of BLMs and biomembranes, however, does not allow long-time monitoring of L-Glutamate, while the GluOx based enzyme sensors (case d) can be applied to long-time monitoring experiments, for example ischemia- or depolarization-induced release of L-glutamate in brain slices. Although the response time of GluOx-based membrane for L-glutamate (case e) is slower as compared with the GluR-based sensors, where the response time is in principle in the range of several ms. However, the potentiality of simultaneous multi-site detection of glutamate may surpass the drawback.

The new approaches described above demonstrated that the appropriate design of GluRs and GluOx systems is useful for the sensing of L-glutamate released in acute brain slices. The agreements between the *in vivo* and *in vitro* results and also between the *in vitro* results indicate that the accurate quantification of L-glutamate can be obtained by the methods. However, it is emphasized that from the methodological viewpoints, the agreement of the results between different methods, in general, means the accuracy of each method, only if glutamate concentration is sufficiently larger than the detection limits of each method. If the concentration of L-glutamate released from a target neuronal region is lower than the detection limit of the method, the sensing system, in principle, does not give rise to any responses to L-Glutamate. This does not mean "no release" of L-Glutamate, but it

Table 4. Comparison of L-glutamate-Sensing Methods Described in this Review

Analytical signal	Concentration range	Response time	Reproducibility (relative standard deviation)	Suitable application
(a) BLM sensors based on multi GluR channels				
Integrated current	0.10 nM-1 μM	<1 min	variable among BLMs	highly sensitive *ex situ* detection
(b) BLM sensors based on single GluR channel				
Integrated current	1-3 μM	<1 min	12% (50 μM)	*ex situ* detection
(c) Biological membrane sensors based on multi GluR channels				
Integrated current	0.5 -5 μM	<1 min	12% (0.75 μM)	sensitive *in situ* detection in neuronal samples
(d) Glass capillary sensors based on GluOx				
Reduction current	1-150 μM	~1 min	23% (50 μM)	*in situ* detection in neuronal samples long-time monitoring
(e) GluOx-based membranes for L-glutamate imaging				
Green dye formation	0.10-4 mM 2.8-8.3 nmol cm^{-2} min^{-1}	9 s	22% (2.8 nmol cm^{-2} min^{-1})	multi-point *in situ* detection under intense stimulation

means the concentration is simply below the detection limit of the sensing method. The biological system with respect to L-glutamate is likely to be active even when its concentration is lower than the detection limit of the sensing method. Consequently, caution is necessary if one wants to draw a conclusion from "non-response".

REFERNCES

[1] Bliss, T. V. P.; Collingridge, G. L. *Nature*, **1993**, *361*, 31.
[2] Nishizawa, Y. *Life Sci*., **2001**, *69*, 369.
[3] Krogsgaard-Larsen, P.; Ebert, B.; Johansen, T. N.; Bischoff, F.; Madsen, U. In *Excitatory Amino Acids and Synaptic Trans*mission, *2nd eds*, Wheal, H. V.: Thomson, A. M., Eds.; Academic Press: London, **1995**; pp. 41-59.
[4] Dingledine, R.; Borges, K.; Bowie, D.; Traynelis, S. F. *Pharmacol. Rev.,* **1999**, 51, 7.
[5] Sugawara, M.; Hirano, A. In *Advances in Planar Lipid Bilayers and Liposomes Volume 1*, Tien, H. T.: Ottova-Leitmannova, A., Eds.; Elsevier Academic Press: Amsterdam, **2005**; pp. 221-245.
[6] Albery, W. J.; Boutelle, M. G.; Galley P. T.; *J. Chem. Soc. Chem. Commun*., **1992**, 900.
[7] Walker, M. C.; Galley, P. T.; Errington, M. L.; Shorvon, S. D.; Jefferys, J. G. R. *J. Neurochem*., **1995**, *65*, 725.
[8] Niwa, O.; Horiuchi, T.; Torimitsu, K. *Biosens. Bioelectron*., **1997**, *12*, 311.
[9] Castillo, J.; Blöchl, A.; Dennison, S.; Schuhmann, W.; Csöregi, E. *Biosens. Bioelectron.*, **2005**, *20*, 2116.
[10] Ly, A. M.; Michaelis, E. K. *Biochemistry*, **1991**, *30*, 4307.
[11] Minami, H.; Sugawara, M.; Odashima, K.; Umezawa, Y.; Uto, M.; Michaelis, E. K.; Kuwana, T. *Anal. Chem*., **1991**, *63*, 2787.
[12] Uto, M.; Michaelis, E. K.; Hu, I. F.; Umezawa, Y.; Kuwana, T. *Anal. Sci*., **1990**, 6, 221.
[13] Sugawara, M.; Hirano, A.; Rehák, M.; Nakanishi, J.; Kawai, K.; Sato, H.; Umezawa, Y. *Biosens. Bioelectron*., **1997**, *12*, 425.
[14] Hirano, A.; Sugawara, M.; Umezawa, Y.; Uchino, S.; Nakajima-Iijima, S. *Biosens. Bioelectron.*, **2000**, *15*, 173.
[15] Laurie, D. J.; Seeburg, P. H. *Eur. J. Pharmacol.*, **1994**, *268*, 335.
[16] Olverman, H. J.; Jones, A. W.; Mewett, K. N.; Watkins, J. C. *Neuroscience*, **1988**, *26*, 17.
[17] Patneau, D. K.; Mayer, M. L. *J. Neurosci.*, **1990**, *10*, 2385.
[18] Ishii, T.; Moriyoshi, K.;, Sugihara, H.; Sakurada, K.; Katodani, H.; Yokoi, M.; Akazawa, C.; Shigemoto, R.; Mizuno, N.; Masu, M.; Nakanishi, S. *J. Biol. Chem*., **1993**, *268*, 2836.
[19] Hirano, A.; Wakabayashi, M.; Sugawara, M.; Uchino, S.; Nakajima-Iijima, S. *Anal. Biochem*., **2000**, *283*, 258.
[20] Wakabayashi, M.; Hirano, A.; Sugawara, M.; Uchino, S.; Nakajima-Iijima, S. *J. Pharm. Biomed. Anal.*, **2001**, *24*, 453.
[21] Kawai, M.; Horikawa, Y.; Ishihara, T.; Shimamoto, K.; Ohfune, Y. *Eur. J. Pharmacol.*, **1992**, *211*, 195.
[22] Mori, H.; Mishina, M. *Neuropharmacology*, **1995**, *34*, 1219.
[23] Kutsuwada, T.; Kashiwabuchi, N.; Mori, H.; Sakimura, K.; Kushiya, E.; Araki, K.; Meguro, H.; Masaki, H.; Kumanishi, T.; Arakawa, M.; Mishina, M. *Nature*, **1992**, *358*, 36.
[24] Vicini, S.; Wang, J. F.; Li, J. H.; Zhu, W. J.; Wang, Y. H.; Luo, J. H.; Wolfe, B. B.; Grayson, D. R. *J. Neurophys*., **1998**, *79*, 555.
[25] Stern, P.; Béhé, P.; Shoepfer, R.; Colquhoun, D. *Proc. R. Soc. Lond. Ser. B*, **1992**, *250*, 271.
[26] Cull-Candy, S.; Brickley, S.; Farrant, M. *Curr. Opin. Neurobiol.*, **2001**, *11*, 327.
[27] Ikeda, K.; Nagasawa, M.; Mori, H.; Araki, K.; Sakimura, K.; Watanabe, M.; Inoue, Y.; Mishina, M. *FEBS Lett.*, **1992**, *313*, 34.
[28] Erreger, K.; Dravid, S. M.; Banke, T. G.; Wyllie, D. J. A.; Traynelis, S. F. *J. Physiol.*, **2005**, *563*, 345.
[29] Liu, L.; Wong, T. P.; Pozza, M. F.; Lingenhoehl, K.; Wang, Y.; Sheng, M.; Auberson, Y. P.; Wang, Y. T. *Science*, **2004**, *304*, 1021.
[30] Massey, P. V.; Johnson, B. E.; Moult, P. R.; Auberson, Y. P.; Brown, M. W.; Molnar, E.; Collingridge, G. L.; Bashir, Z. I. *J. Neurosci*., **2004**, *24*, 7821.
[31] Yoshimura, Y.; Ohmura, T.; Komatsu, Y. *J. Neurosci.*, **2003**, *23*, 6557.
[32] Maeda, T.; Shimoshige, Y.; Mizukami, K.; Shimohama, S.; Kaneko, S.; Akaike, A.; Satoh, M. *Neuron*, **1995**, *15*, 253.
[33] Maeda, T.; Kaneko, S.; Akaike, A.; Satoh, M. *Neurosci. Lett*., **1997,** *224*, 103.
[34] O'Connor, J. J.; Wu, J.; Rowan, M. J.; Anwyl, R. *Neuroscience*, **1995**, *69*, 363.
[35] Rossi, D. J.; Oshima, T.; Attwell, D. *Nature*, **2000**, *403*, 316.
[36] Shimane, M.; Miyagawa, K.; Sugawara, M. *Anal Biochem.*, **2006**, *353*, 83.
[37] Knott,C.; Maguire, J. J.; Moratalla, R.; Bowery, N. G. *Neuroscience*, **1993**, *52*, 73.
[38] Kasai, N.; Jimbo, Y.; Niwa, O.; Matsue, T.; Torimitsu, K. *Neurosci. Lett*., **2001**, *304*, 112.
[39] Schmidt-Kastner, R.; Freund, T. F. *Neuroscience,* **1991**, *40*, 599.
[40] Manabe, T. *Rev. Neurosci*., **1997**, *8*, 179.
[41] Tsien, R. Y. *Ann. Rev. Neurosci*., **1989**, *12*, 227.
[42] Regehr, W. G.; Connor, J. A.; Tank, D. W. *Nature,* **1989**, *341*, 533.
[43] Miyawaki, A.; Llopis, J.; Heim, R.; MaCaffery, J. M.; Adams, J. A.; Ikura, M.; Tsien, R. Y. *Nature*, **1997**, *388*, 882.
[44] Hempel, C. M.; Vincent, P.; Adams, S. R.; Tsien, R. Y.; Selverston, A. I. *Nature*, **1996**, *384*, 166.
[45] Sato, M.; Hida, N.; Ozawa, T.; Umezawa, Y. *Anal. Chem*., **2000**, *72*, 5918.
[46] Kojima, H.; Nakatsubo, N.; Kikuchi, K.; Kawahara, S.; Kirino, Y.; Nagoshi, H.; Hirata,Y.; Nagano, T. *Anal. Chem.*, **1998**, *70*, 2446.
[47] Ozawa, T.; Nogami, S.; Sato, M.; Ohya, Y,; Umezawa, Y. *Anal. Chem*., **2000**, *72*, 5151.
[48] Parpura, V.; Tong, W.; Yeung, E. S.; Haydon, P. G. *J. Neurosci. Methods*, **1998**, *82*, 151.
[49] Lillard, S. J.; Yeung, E. S. *J. Neurosci. Methods*, **1997**, *75*, 103.
[50] Qian, W.-J.; Aspinwall, C. A.; Battiste, M. A.; Kennedy, R. T. *Anal. Chem*., **2000**, *72*, 711.
[51] Gee, K. R.; Zhou, Z.-L.; Qian, W.-J.; Kennedy, R. *J. Am. Chem. Soc*., **2002**, *124*, 776.
[52] Mitani, A.; Kadoya, F.; Nakamura, Y.; Kataoka, K. *Neurosci. Lett*., **1991**, *122*, 167.
[53] Uchino, S.; Nakamura, T.; Nakamura, K.; Nakajima-Iijima, S.; Mishina, M.; Kohsaka, S.; Kudo, Y. *Eur. J. Neurosci.*, **2001**, *13*, 670.
[54] Kasai, N.; Jimbo, Y.; Torimitsu, K. *Anal. Sci.,* 2002, *18*, 1325.
[55] Hirano, A.; Asakawa, M.; Kido, N.; Sugawara, M. *Anal. Sci.*, **2000**, *16*, 25.
[56] Hirano, A.; Moridera, N.; Akashi, M.; Saito, M.; Sugawara, M. *Anal. Chem*., **2003**, *75*, 3775.
[57] Lipton, P. *Physiol. Rev.,* **1999**, *79*, 1431.
[58] White, B. C.; Sullivan, J. M.; DeGracia, D. J., O'Neil, B. J.; Neumar, R. W.; Grossman, L. I.; Rafols, J. A.; Krause, G. S. *J. Neurol. Sci*., **2000**, *179*, 1.
[59] Zhou, S. Y.; Zuo, H.; Stobaugh, J. F.; Lunte, C. E.; Lunte, S. M. *Anal. Chem*., **1995**, *67*, 594.
[60] Rowley, H. L.; Martin, K. F. Marsden, C. A. *J. Neurosci. Methods*, **1995**, *57*, 93.
[61] Zilkha, E.; Obrenovitch, T. P.; Koshy, A. Kusakabe, H.; Bennetto, H. P. *J. Neurosci. Methods*, **1995**, *60*, 1.
[62] Jay, T. M.; Zilkha, E.; Obrenovitch, T. P. *J. Neurophysiol.*, **1999**, *81*, 1741.
[63] Errington, M. L.; Galley, P. T.; Bliss, T. V. P. *Phil. Trans. R. Soc. Lond. B*, **2003**, *358*, 675.
[64] Niwa, O.; Torimitsu, K.; Morita, M.; Osborne, P.; Yamamoto, K. *Anal. Chem*., **1996**, *68*, 1865.
[65] Nakajima, K.; Yamagiwa, T.; Hirano, A.; Sugawara, M. *Anal. Sci.*, **2003**, *19*, 55.
[66] Nakamura, N.; Negishi, K.; Hirano, A.; Sugawara, M. *Anal. Bioanal. Chem.*, **2005**, *383*, 660.
[67] Asai, S.; Iribe, Y.; Kohno, T.; Ishikawa, K. *NeuroReport*, **1996**, *7*, 1092.
[68] Kohno, T.; Asai, S.; Iribe, Y.; Hosoi, I.; Shibata, K. Ishikawa, K. *J. Neurosci. Methods*, **1998**, *81*, 199.
[69] Kusakabe, H.; Midorikawa, Y.; Kuninaka, A.; Yoshino, H. *Agric. Biol. Chem.*, **1983**, *47*, 179.
[70] Vreeke, M.; Maiden, R.; Heller A. *Anal. Chem*., **1992**, *64*, 3084.
[71] Hu, Y.; Mitchell, K. M.; Albahadily, F. N.; Michaelis, E. K.; Wilson, G. S. *Brain Res.*, **1994**, *659*, 117.
[72] Kulagina, N. V.; Shankar, L.; Michael, A. C. *Anal. Chem*., **1999**, *71*, 5093-5100.
[73] Bergles, D. E.; Jahr, C. E. *Neuron*, **1997**, *19*, 1297.
[74] Diamond, J. S.; Bergles, D. E.; Jahr, C. E. *Neuron*, **1998** *21*, 425.

[75] Lüscher, C.; Malenka, R. C.; Nicoll, R. A. *Neuron*, **1998**, *21*, 435.
[76] Akagi, Y.; Hashigasako, A.; Degenaar, P.; Iwabuchi, S.; Hasan, Q.; Morita, Y.; Tamiya, E. *J. Biochem*., **2003**, *134*, 353.
[77] Ayoub, G. S.; Dorst, K. *Vision Res*., **1998**, *38*, 2909.
[78] Ayoub, G. S.; Grutsis, S.; Simko, H. *J. Neruosci. Methods,* **1998**, *81*, 113-119.
[79] Tohda, C.; Kuraishi, Y. *Neurosci. Res.,* **1996**, *24*, 183.
[80] Innocenti, B.; Parpura, V.; Haydon, P. G. *J. Neurosci*., **2000**, *20*, 1800-1808.
[81] Kawamura, Y.; Manita, S.; Nakamura, T.; Inoue, M.; Kudo, Y.; Miyakawa, H. *Eur. J. Neurosci*., **2004**, *19*, 1591.
[82] Okumoto, S.; Looger, L. L.; Micheva, K. D.; Reimer, R. J.; Smith, S. J.; Frommer, W. B. *Proc. Natl. Acad. Sci. USA*, **2005**, *102*, 8740.

Received: December 27, 2005 **Revised: May 08, 2006** **Accepted: May 09, 2006**